Polymer Journal (2018) 50:397–406
https://doi.org/10.1038/s41428-018-0025-y

ORIGINAL ARTICLE

Gel-emulsions prepared using a low-molecular-weight gelator and their use in the synthesis of porous polymers

Yudai Imasaka[1] · Mayu Sano[1] · Masahiro Suzuki[2] · Kenji Hanabusa[2,3]

Received: 9 November 2017 / Revised: 12 January 2018 / Accepted: 15 January 2018 / Published online: 19 February 2018

Abstract

Water-in-oil (W/O) gel-emulsions consisting of water and a monomer were successfully prepared using *N*-3-hydroxypropylcarbonyl-L-isoleucyl-aminooctadecane as a gelator. Low-temperature polymerization of the gel-emulsions with a redox initiator was performed to obtain the corresponding porous polymers. Furthermore, polymerization of gel-emulsions containing bifunctional monomers gave crosslinked porous PMMA-HDODA, PMMA-EGDMA, PMMA-DVB, and PSt-DVB, which were found to be mechanically robust and solvent resistant. The microstructures of the porous polymers and crosslinked porous polymers were observed by scanning electron microscopy. The adsorption capacities of the polymers toward methanol, dichloromethane, acetone, tetrahydrofuran, toluene, hexane, and kerosene were assessed and rationalized in terms of the surface microstructures of the polymers. The time courses of the adsorptions were investigated, revealing a two-step adsorption process comprising rapid permeation into the cavities of the porous polymers followed by a slow swelling step. The high water-repellency of the crosslinked porous polymers was confirmed by contact angle measurement. The reusabilities of the polymers as solvent absorbents were evaluated through repeated adsorption and drying.

Introduction

Recent years have seen increased research interest in low-molecular-weight gelators that can physically gel liquids such as water and organic solvents. They are particularly attractive because large volumes of liquid can be immobilized through self-assembly using very small amounts of the gelator. Consequently, advances in the area of supramolecular chemistry have led to a number of studies on gelators being published in recent years [1–20]. Low-molecular-weight gelators have unique characteristics, including good solubility upon heating and the ability to induce the smooth gelation of liquids. Gelators are characterized by thermally reversible sol-gel transitions because the three-dimensional network structures responsible for gelation are built up through noncovalent interactions such as hydrogen bonding, electrostatic interactions, van der Waals interactions, and π–π interactions. Although gelators are already used as hardeners for cooking oils, cosmetic materials, and thickeners for paint, recent gelator research has focused on their application in fields such as drug delivery and drug release in biomaterials [21–27], scaffold materials for cells in tissue engineering [28, 29], sensors [30–34], templates for the synthesis of inorganic nanostructures [35–39], auxiliary agents for producing organic electronics [12, 40], electrolytes that prevent liquid leakage [41], and detectors for explosives [42–45]. Furthermore, porous materials receive considerable research attention owing to their wide applicability in areas such as adsorption [46, 47], gas storage and separation [48–54], tissue engineering [55–59], drug delivery [60], and catalyst immobilization [61–65].

Electronic supplementary material The online version of this article (https://doi.org/10.1038/s41428-018-0025-y) contains supplementary material, which is available to authorized users.

✉ Kenji Hanabusa
hanaken@shinshu-u.ac.jp

[1] Faculty of Textile Science and Technology, Shinshu University, Ueda 386-8567, Japan

[2] Interdisciplinary Graduate School of Science and Technology, Shinshu University, Ueda 386-8567, Japan

[3] Division of Frontier Fibers, Institute for Fiber Engineering, ICCER, Shinshu University, Ueda 386-8567, Japan

Several studies on the preparation of porous polymers using emulsions have been reported. For example, Tokuyama et al. succeeded in preparing porous poly(*N*-isopropylacrylamide) using oil-in-water (O/W) emulsions stabilized by polyethylene glycol (PEG)-type surfactants [66, 67], Zhou et al. prepared porous polystyrene materials using O/W emulsions stabilized by amphiphilic carbonaceous microspheres [68], and Jiang et al. reported the preparation of poly(styrene-divinylbenzene) foam from high-internal-phase emulsions (HIPEs) stabilized by Span 80 [69]. Fang et al.'s work on gel-emulsions formed by low-molecular-weight gelators and their use in the preparation of porous polymers is particularly interesting. They reported the preparation of porous polymers via the gelation of emulsions containing a cholesteryl derivative of diethanolamine [47] and a polymerizable cholesteryl derivative [70] as low-molecular-weight gelators. However, to the best of our knowledge, Fang's work is the only example of the use of low-molecular-weight gelators to prepare gel-emulsions and their subsequent polymerization.

Over the last two decades, we have developed many low-molecular-weight gelators and studied their applications [8, 37–41, 44, 71]. Herein, we report the preparation of gel-emulsions using a novel low-molecular-weight L-valine-derivative gelator. The successful preparation of porous polymers by the radical polymerization of gel-emulsions and their application as oil absorbents were also investigated.

Experimental

Instrumentation

Elemental analysis was performed with a Perkin-Elmer 240B analyzer. Infrared spectra were recorded on a Jasco FTIR-7300 spectrometer using KBr plate. ^{1}H NMR spectra were recorded on a Bruker AVANCE 400 spectrometer. Scanning electron microscopy (SEM) was done with a Hitachi SU1510. The stirring for preparation of gel-emulsion was performed with an AS ONE Test Tube Mixer HM-2F. Contact angle was measured by a Kyowa Interface Science DMs-400 Contact Angle Meter. Fluorescence microscopy was performed with an Olympus FV10-ASW.

Reagents

Methyl methacrylate (MMA), styrene (St), and γ-butyrolactone were purchased from Wako Pure Chemical Industries, Ltd. Benzoyl peroxide (BPO), divinylbenzene (DVB), 1,6-hexanediol diacrylate (HDODA), ethylene glycol dimethacrylate (EGDMA), 3-ferrocenoylpropionic acid (3-Fepa), and sorbitan monostearate (Span 60) were purchased from Tokyo Chemical Industry Co., Ltd.

Synthesis of *N*-3-hydroxypropylcarbonyl-L-isoleucyl-aminooctadecane

N-Carbobenzyloxy-L-isoleucylaminooctadecane [41] (51.68 g, 0.10 mol) was hydrogenated in the presence of Pd-C in 500 mL of 1-propanol for 5 h at room temperature under a hydrogen atmosphere. After confirming the complete removal of protecting group by TLC (chloroform: methanol: acetic acid = 95:5:1 as volume ratio), the solution was filtered off. The filtrate was evaporated and recrystallized from 300 mL of ligroin to provide 35.3 g (92%) of L-isoleucylaminooctadecane. A mixture of 6.50 g (17 mmol) of L-isoleucyl-aminooctadecane and 1.46 g (17 mmol) of γ-butyrolactone in 60 mL of dry THF was refluxed overnight under an argon atmosphere. After evaporating, the crude product was recrystallized from 50 mL of ethyl acetate. *N*-3-hydroxypropylcarbonyl-L-isoleucyl-aminooctadecane was obtained in a yield of 5.1 g (64%). The product was recrystallized again from methanol for elemental analyses. IR (KBr, cm^{-1}): 3380 (νOH), 3301 (νNH), 1639 (νC=O amide I), 1552 (δN–H amide II). Found: C 72.11, H 11.79, N 6.15%. Calcd for $C_{28}H_{56}N_2O_3$: C 71.74, H 12.04, N 5.98%. ^{1}H-NMR (400 MHz, $CDCl_3$, TMS, 25 °C): $\delta = 0.86$–0.97 (m, 9H, C$\underline{H_3}$), 1.25 (br, 32H, alkyl), 1.49–2.06 (m, 6H, CONHCH$_2$C$\underline{H_2}$, HOCH$_2$C$\underline{H_2}$, C$\underline{H_2}$CONH), 2.33–2.45 (m, 1H, C$\underline{H}$(CH$_3$)(CH$_2$CH$_3$)), 3.14–3.33 (m, 2H, CONHC$\underline{H_2}$), 3.67–3.72 (m, 2H, HOC$\underline{H_2}$), 4.20 (t, $J = 8.10$, 1H, CONHC$\underline{H}$CONH), 6.00 (t, $J = 5.24$, 1H, CON$\underline{H}$CH$_2$), 6.43 (d, $J = 8.84$, 1H, CON$\underline{H}$CH).

Preparation of gel-emulsion

Gel-emulsions were prepared as follows: A mixture of the weighed gelator, monomer, and Span 60 in a test tube was heated until the solid dissolved. A predetermined amount of water was added to the resulting solution and stirred vigorously by a test tube mixer. After standing at 25 °C for 2 h, the formation of gel-emulsion was checked visually. When no fluid ran down the wall of the test tube upon inversion of the test tube, we judged it to be gel-emulsion.

Polymerization of gel-emulsion

A mixture of the weighed gelator, monomer, Span 60, and 3-Fepa in a test tube was heated until the solid dissolved. A predetermined amount of water was added to the solution and

stirred vigorously at room temperature to form a gel-emulsion. BPO was added to the gel-emulsion while stirring

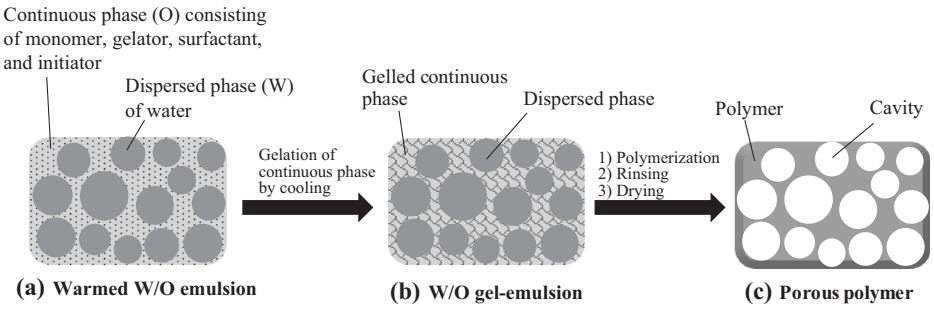

Fig. 1 Concept of preparation of porous polymers from gel-emulsion. (Color figure online)

and then left to stand at 40 °C overnight. Polymerized matter was taken out by breaking the test tube and washed with methanol to remove unreacted monomer, gelator, Span 60, and 3-Fepa.

Organic liquid adsorption test

To estimate the maximum adsorption capacity of the porous polymer, a porous polymer with known weight was placed in a beaker filled with a liquid. After 30 min of adsorption, the wet porous polymer was drained for 5 min until no residual droplets were left on the surface. The adsorption capacity was calculated by the following formula. The q is the adsorption capacity (mL g^{-1}), m_s is the weight of the wet porous polymer after 5 min of drainage (g), m_0 is the initial weight of the porous polymer (g), and d is the density of the liquid.

Results and discussion

Porous polymers

Figure 1 illustrates the concept of preparation of porous polymers from gel-emulsions. Figure 1a shows a warmed W/O emulsion in which "W" indicates the dispersed water phase and "O" indicates the continuous oily monomer phase, which contains the gelator, surfactant, and initiator. Gentle heating is necessary to dissolve the gelator in the continuous phase. Figure 1b illustrates a gel-emulsion formed upon cooling the warmed W/O emulsion to room temperature, in which the continuous phase "O" is gelled by the gelator. Low-temperature redox polymerization proceeds in the gelled continuous phase of the gel-emulsion to form a polymerized gel-emulsion. Figure 1c illustrates the porous polymer after removing the gelator, Span 60, and 3-Fepa by rinsing. The dispersed water phase shown in Fig. 1b imparts cavities to the porous polymer, as shown in Fig. 1c. Thus, porous polymers prepared from gel-emulsions with high aqueous phase fractions (APFs) possess many cavities and exhibit low density.

The preparation of a porous polymer is illustrated in Fig. 2. The process consists of the following four steps: (1) the formation of an isotropic solution containing the gelator, Span 60, 3-Fepa, and monomer upon heating; (2) the addition of water; (3) stirring and the addition of the benzoyl peroxide (BPO) initiator followed by standing at 40 °C overnight; and (4) rinsing the polymer with methanol.

In this study, *N*-3-hydroxypropylcarbonyl-L-isoleucyl-aminooctadecane and Span 60 were used as the gelator and surfactant, respectively (Fig. 2). Both gelator and surfactant are indispensable in the preparation of stable gel-emulsions, with the surfactant being responsible for emulsification and the gelator being responsible for gelation of the emulsion. The gel-emulsions formed were so stable that no separation or collapse occurred, even after several months. The gelator is insoluble in water. Therefore, only the oily monomer layer in the emulsion undergoes gelation. The minimum gelator concentrations required to form gels at 25 °C from typical liquids are 40 g L^{-1} for methyl methacrylate (MMA), 10 g L^{-1} for styrene (St), 4 g L^{-1} for dodecane, 30 g L^{-1} for toluene, 20 g L^{-1} for dimethyl sulfoxide (DMSO), 10 g L^{-1} for propylene carbonate, 10 g L^{-1} for isopropyl myristate, 4 g L^{-1} for silicone oil, and 4 g L^{-1} for ethylene glycol. The compositions of gel-emulsions with APFs of 90, 85, and 80 vol% are summarized in Table 1. BPO and 3-Fepa were added to these emulsions as redox initiators for low-temperature polymerization. The addition of a small amount of the gelator and Span 60, ca. 4.2 wt% against the monomer, was sufficient to form gel-emulsions. The gel-emulsions were composed of water and MMA (or St), and the oil phase was gelled by the gelator. The gel-emulsions formed were confirmed to be W/O-type by fluorescence microscopy images (Fig. S1) using bis(hexadecyloxy) fluorescein [71], which dyes the oil phase orange.

Figure 3 shows the SEM images of the porous PMMA obtained via polymerization of the gel-emulsions with the compositions shown in Table 1. It should be noted that the gelator, Span 60, and 3-Fepa were completely removed from the polymers upon rinsing with methanol, as evidenced by the complete absence of νC=O stretching vibrations for the gelator (1640 cm^{-1}), Span 60 (1738 cm^{-1}), and 3-Fepa (1714 cm^{-1}) from the FT-IR spectra of the

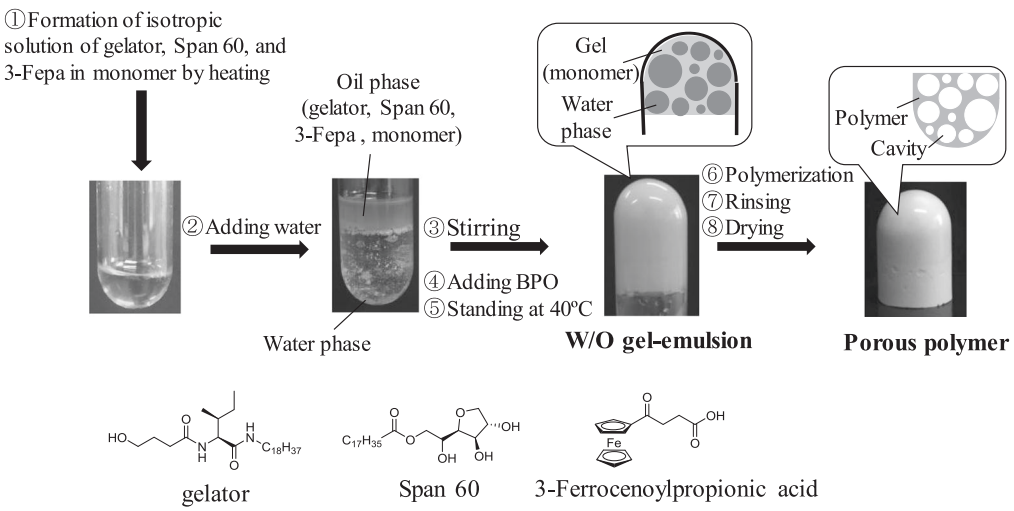

Fig. 2 Preparation process of porous polymer. (Color figure online)

Table 1 Compositions of gel-emulsions for preparation of porous PMMAs

APFs (vol-%)	Water (ml)	MMA (ml)	Gelator (mg)	Span 60 (mg)	3-Fepa (mg)	BPO (mg)
90	3.6	0.4	16	16	1.7	1.5
85	3.4	0.6	24	24	2.6	2.2
80	3.2	0.8	32	32	3.4	3.0

APFs aqueous phase fractions, *MMA* methyl methacrylate, *Span 60* sorbitan monostearate, *3-Fepa* 3-ferrocenoylpropionic acid, *BPO* benzoyl peroxide

porous polystyrene (PSt) samples after rinsing (see Fig. S2 for porous PMMA' IR spectrum). It is clear from the images in Fig. 3 that the porous PMMAs comprise spherical structures whose diameters are several tens of micrometers and that their walls are brittle and partially broken. The spherical structures have internal cavities, and the densities of the porous PMMAs were 0.19 g cm^{-3} (APF 80 vol%), 0.14 g cm^{-3} (APF 85 vol%), and 0.11 g cm^{-3} (APF 90 vol %). The adsorption capacities of the porous PMMA materials toward kerosene increase with increasing APF. The adsorption capacities after 30 min are 1.4 mL g^{-1} (APF 80 vol%), 2.7 mL g^{-1} (APF 85 vol%), and 4.0 mL g^{-1} (APF 90 vol%). The adsorption capacities of PMMA (APF 90 vol %) toward methanol, toluene, and hexane are 11.6, 5.76, and 3.51 mL g^{-1}, respectively. However, all of the porous PMMAs dissolve in dichloromethane, acetone, and THF within 30 min.

Crosslinked porous PMMAs

In order to improve the solvent resistances of the porous PMMAs, we attempted crosslinking using bifunctional vinyl monomers. The compositions of the gel-emulsions used for the preparation of crosslinked porous PMMAs are given in Table 2, where the amounts of 1,6-hexanediol diacrylate (HDODA), ethylene glycol dimethylacrylate (EGDMA), and divinylbenzene (DVB) are 0.2 molar equivalents with respect to MMA.

Figure 4 shows the SEM images of the crosslinked porous PMMA–HDODA obtained by polymerization of gel-emulsions containing HDODA. The spherical diameters of the crosslinked porous PMMA–HDODA particles are several tens of micrometers, and they increase with increasing APF. Because the gel-emulsions are of the W/O-type, a high APF results in the formation of large spherical structures. The spherical structures seem robust and independent compared to those shown in Fig. 3. Indeed, crosslinked porous PMMA–HDODA does not collapse under finger pressure, unlike the porous PMMAs. The densities of PMMA–HDODA, PMMA–EGDMA, and PMMA–DVB prepared at an APF of 90 vol% are 0.11, 0.092, and 0.078 g cm^{-3}, respectively. The adsorption capacities of PMMA–HDODA toward kerosene are 0.4 mL g^{-1} (APF 80 vol%), 1.1 mL g^{-1} (APF 85 vol%), and 2.8 mL g^{-1} (APF 90 vol%). Although crosslinking by HDODA decreases adsorption capacity as compared to those of the porous PMMAs, they successfully absorb dichloromethane, acetone, and THF owing to their solvent resistances (Fig. 5). Thus, although solvent resistance and mechanical strength can be improved by crosslinking, the spherical structures are so robust that they possibly do not absorb solvents on the inside.

To study the effects of the crosslinking agents on adsorption capacity, we substituted HDODA with EGDMA or DVB (Table 2). Figure 6 shows the SEM images of crosslinked porous PMMA–HDODA, PMMA–EGDMA,

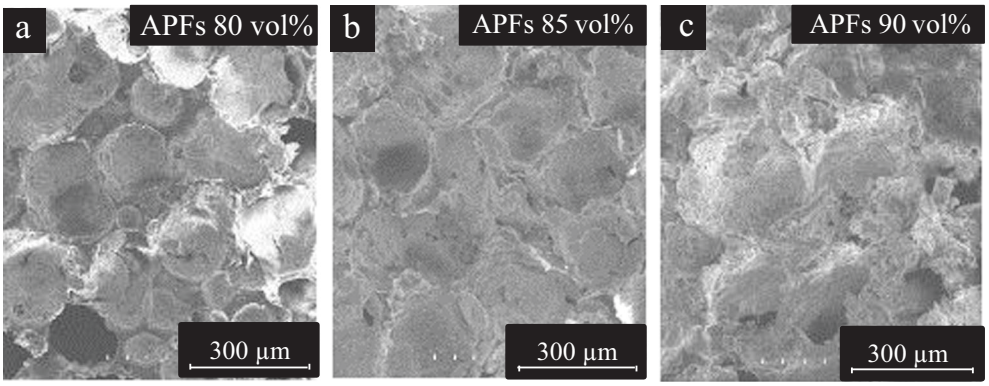

Fig. 3 SEM images of the porous composite monoliths produced by using the gel emulsion. **a** APFs 80 vol%—water/MMA. **b** APFs 85 vol%—water/MMA. **c** APFs 90 vol%—water/MMA. APFs aqueous phase fractions

Table 2 Compositions of gel-emulsions for preparation of crosslinked porous PMMAs

APFs (vol-%)	Water (ml)	MMA (ml)	Crosslinking agent (ml)	Gelator (mg)	Span 60 (mg)	3-Fepa (mg)	BPO (mg)
90	3.6	0.333	0.067 (HDODA)	16	16	1.7	1.5
85	3.4	0.50	0.10 (HDODA)	24	24	2.6	2.2
80	3.2	0.67	0.13 (HDODA)	32	32	3.4	3.0
90	3.6	0.333	0.067 (EGDMA)	16	16	1.7	1.5
90	3.6	0.333	0.067 (DVB)	16	16	1.7	1.5

HDODA 1,6-hexanediol diacrylate, *EGDMA* ethylene glycol dimethacrylate, *DVB* divinylbenzene

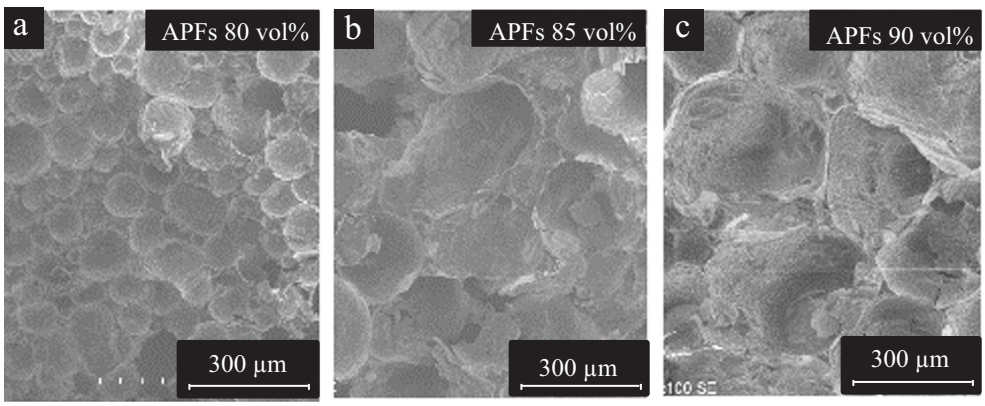

Fig. 4 SEM images of the porous composite monoliths produced by using the gel emulsion. **a** APFs 80 vol%—water/MMA and HDODA. **b** APFs 85 vol%—water/MMA and HDODA. **c** APFs 90 vol%—water/MMA and HDODA

and PMMA–DVB. The image of PMMA–EGDMA is very similar to that of PMMA–HDODA in that the size of the spherical structures is several tens of micrometers and their walls are independent and robust. In contrast, the spherical surfaces of the PMMA–DVB particles are characterized by many cracks. The adsorption capacities of PMMA–HDODA, PMMA–EGDMA, and PMMA–DVB toward methanol, dichloromethane, acetone, THF, toluene, hexane, and kerosene are shown in Fig. 7. The order of adsorption capacities is PMMA–DVB > PMMA–HDODA > PMMA–EGDMA. The high adsorption capacity of PMMA–DVB may be attributed to the cracks in the spherical surfaces. The formation of cracks is unclear at this time, but they will be formed by shrinking associated with the polymerization.

The time courses of the adsorption of kerosene (Fig. 8a) and toluene (Fig. 8b) were obtained. The adsorption capacities after 5 s kerosene adsorption are 0.64 mL g^{-1}

(PMMA–HDODA), 1.6 mL g^{-1} (PMMA–EGDMA), and 4.3 mL g^{-1} (PMMA–DVB). This indicates that PMMA–HDODA, PMMA–EGDMA, and PMMA–DVB absorb kerosene almost instantly. In the case of toluene (Fig. 8b), the adsorption capacities after 5 s are 1.3 mL g^{-1} (PMMA–HDODA), 0.93 mL g^{-1} (PMMA–EGDMA), and 2.0 mL g^{-1} (PMMA–DVB). When the immersion time is extended, the adsorption capacities drastically increase. The large adsorption capacities upon extended immersion are due to the swelling effect. The volume of PMMA–HDODA after 3 days of adsorption is 1.9 times its original volume. The results shown in Fig. 8 indicate that the adsorption of solvents proceeds via two steps: rapid permeation into the cavities of the porous polymers and a subsequent slow swelling, which is a characteristic of crosslinked polymers. The swelling aspects of crosslinked PMMAs before and after adsorbing kerosene and toluene are shown in Figs. S3 and S4.

Crosslinked porous PSt

We also prepared crosslinked porous polymers using St instead of MMA. The compositions of the gel-emulsions for APFs of 90, 85, and 80 vol% are similar to those in Table 2, except for the monomer. Figure 9 shows the SEM images of crosslinked porous PSt–DVB obtained from polymerization of the gel-emulsions. The spherical structures in PSt–DVB are smaller than those in the crosslinked porous PMMAs, and many holes are observed on their surfaces. The densities of PSt–DVB are 0.19 g cm^{-3} (APF 80 vol%), 0.14 g cm^{-3} (APF 85 vol%), and 0.078 g cm^{-3} (APF 90 vol%). The adsorption capacities of PSt–DVB toward kerosene after 30 min are 2.8 mL g^{-1} (APF 80 vol%), 4.1 mL g^{-1} (APF 85 vol%), and 10.0 mL g^{-1} (APF 90 vol%). Figure 10 shows the adsorption capacities of PSt–DVB (APF 90 vol %) toward methanol, dichloromethane, acetone, THF, toluene, hexane, and kerosene. In all solvents, the adsorption capacities are higher compared with those of PMMA–DVB (cf. Fig. 5). When PSt–DVB (APF 90 vol%) is immersed in kerosene for 5 s, the adsorption capacity is 8.8 mL g^{-1}, which is two times that of PMMA–DVB (Fig. S5). The rapid adsorption by PSt–DVB is thought to be due to the high porosity ($d = 0.078$ g cm^{-3}) and the small spherical structures with many holes. It is thought that contact zones between the dispersed water phase in the gel-emulsion remained as holes on polymer surface.

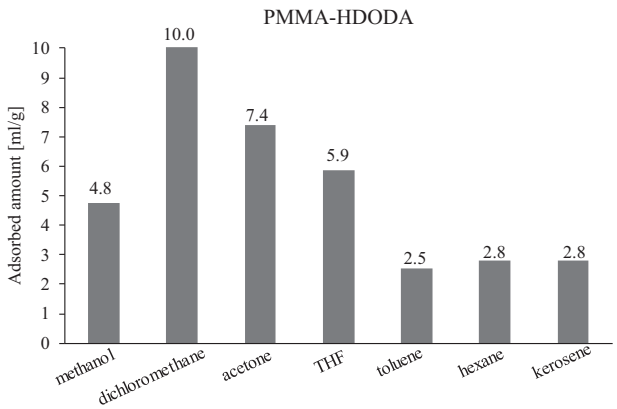

Fig. 5 Adsorption capacities of monolith. APFs 90 vol% PMMA-HDODA

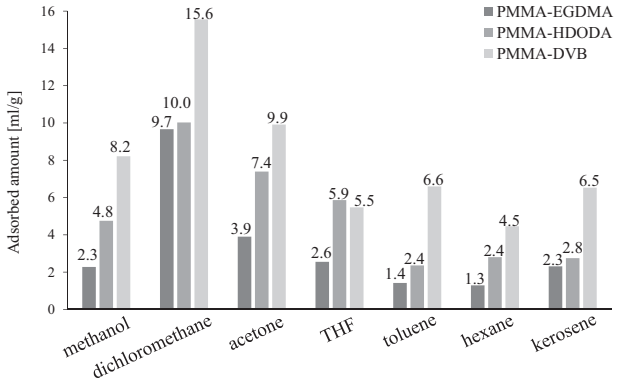

Fig. 7 Adsorption capacities of the monolith. APFs 90 vol% PMMA-EGDMA, APFs 90 vol% PMMA-HDODA, APFs 90 vol% PMMA-DVB. APFs aqueous phase fractions

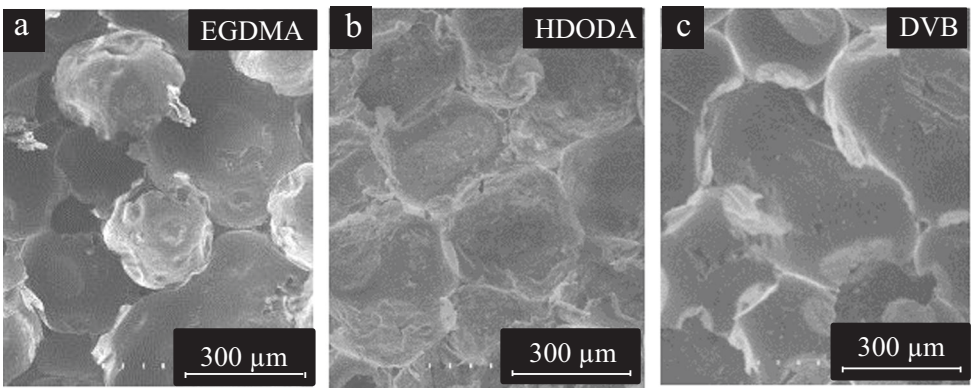

Fig. 6 SEM images of the porous composite monoliths produced by using the gel emulsion. **a** APFs 90 vol%—water/MMA and EGDMA. **b** APFs 90 vol%—water/MMA and HDODA. **c** APFs 90 vol% —water/MMA and DVB

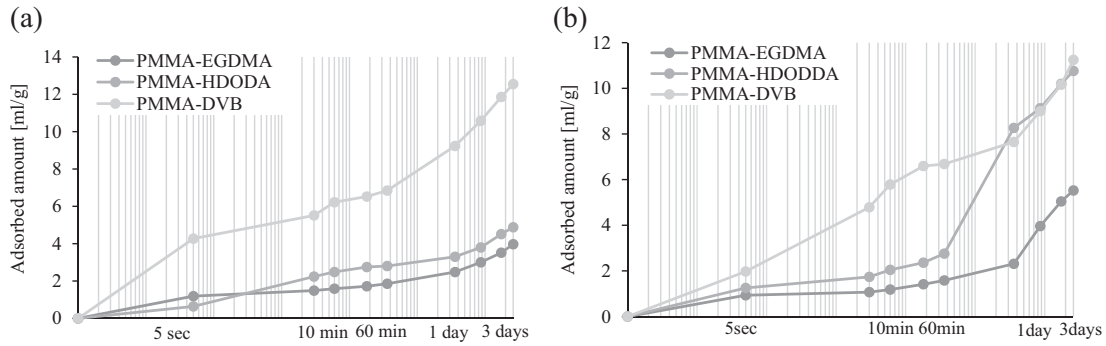

Fig. 8 **a** Adsorption capacity of the materials to kerosene as function of time. **b** Adsorption capacity of the materials to toluene as function of time

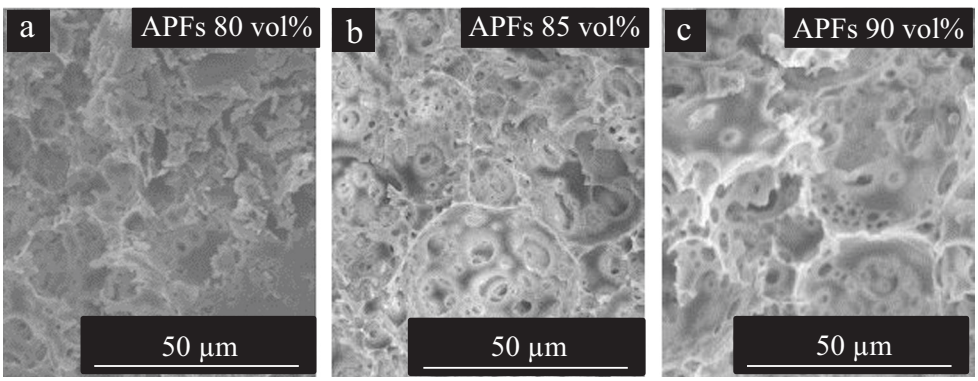

Fig. 9 SEM images of the porous composite monoliths produced by using the gel emulsion. **a** APFs 80 vol%—water/St and DVB. **b** APFs 85 vol%—water/St and DVB. **c** APFs 90 vol%—water/St and DVB

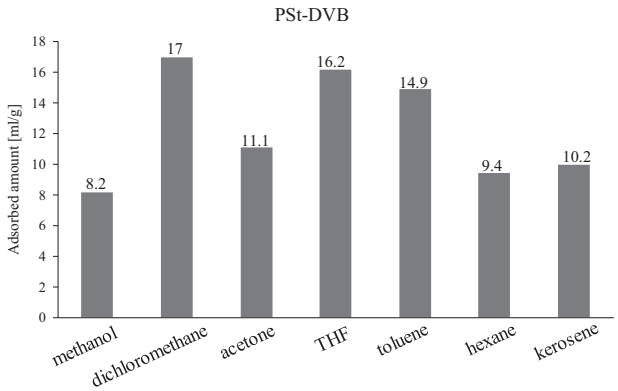

Fig. 10 Adsorption capacities of the monolith. APFs 90 vol% PSt-DVB

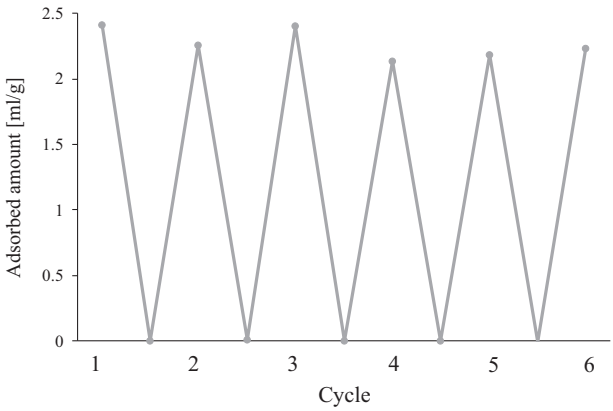

Fig. 11 Reversibility of PMMA–HDODA for adsorption processes against kerosene. APFs 90 vol%

Water-repellency and absorbent reusability

The water contact angles of the crosslinked porous polymers were measured to investigate their water-repellencies. The contact angles of PMMA–HDODA, PSt–DVB, and PMMA–DVB (APF 90 vol%) are 117.3°, 125.4°, and 117.0°, respectively (Fig. S6), confirming their high water-repellencies, which are most likely due to the unevenness of their surfaces. The high water-repellencies allow these crosslinked porous polymers to recover oils from water easily.

The reusability of PMMA–HDODA as a kerosene absorbent was evaluated by repeated adsorption and drying cycles. As shown in Fig. 11, the adsorption/recovery cycle can be repeated several times with very little impact on capacity (see Fig. S7 for reversibility of adsorption processes of porous PMMA).

Conclusion

W/O-type gel-emulsions consisting of water and a monomer were prepared using *N*-3-hydroxypropylcarbonyl-L-isoleucyl-aminooctadecane as a gelator and Span 60 as a surfactant. Low-temperature polymerization of the gel-emulsions with a redox initiator gave the corresponding porous polymers with low densities. The porous PMMAs have spherical structures with internal cavities, and their walls are brittle and partially broken. The adsorption capacities of the porous PMMAs toward kerosene increase with increasing APF.

Robust crosslinked porous PMMAs showing solvent resistance were obtained by the polymerization of gel-emulsions containing bifunctional monomers. The crosslinked porous PMMA–HDODA adsorbs methanol, dichloromethane, acetone, THF, toluene, hexane, and kerosene. The walls of the spherical structures in PMMA–HDODA and PMMA–EGDMA are independent and robust. In contrast, the spherical surfaces in PMMA–DVB contain many cracks. The adsorption capacities are in the order PMMA–DVB > PMMA–HDODA > PMMA–EGDMA. The time courses of the adsorption by the crosslinked porous PMMAs revealed that the adsorption of solvents proceeds through two steps: rapid permeation into the cavities of porous polymers and a subsequent slow swelling, which is a characteristic of crosslinked polymers.

The spherical structures in crosslinked porous PSt–DVB are smaller than those in the crosslinked porous PMMAs, and many holes were observed on the surfaces of the porous PSt–DVB particles. The adsorption capacities of PSt–DVB are higher than those of PMMA–DVB.

The high water-repellencies of the crosslinked porous polymers were confirmed. The adsorption/recovery process could be repeated several times, and the processes were essentially reversible. The extreme lightness, high water-repellency, and reusability of the crosslinked porous polymers indicate that they are especially promising as oil-removing absorbents.

Acknowledgements The present research was supported in part by JSPS KAKENHI Grant Number JP15K05623.

Compliance with ethical standards

Conflict of interest The authors declare that they have no conflict of interest.

References

1. Terech P, Weiss RG. Low-molecular mass gelators of organic liquids and the properties of their gels. Chem Rev. 1997;97:3133–59.
2. Esch JH, Feringa BL. New functional materials based on self-assembling organogels: From serendipity towards design. Angew Chem Int Ed. 2000;39:2263–6.
3. Estroff LA, Hamilton AD. Water gelation by small organic molecules. Chem Rev. 2004;104:1201–17.
4. Fages F. Low molecular mass gelators: design, self-assembly, function. Berlin: Springer; 2005.
5. Terech P, Weiss RG. Weiss, Molecular gels, materials with self-assembled fibrillar networks. Dordrecht: Springer; 2006.
6. Dastidar P. Supramolecular gelling agents: can they be designed? Chem Soc Rev. 2006;37:2699–715.
7. Banerjee S, Das RK, Maitra U. Supramolecular gels 'in actin'. J Mater Chem. 2009;19:6649–87.
8. Suzuki M, Hanabusa K. Polymer organogelators that make supramolecular organogels through physical cross-linking and self-assembly. Chem Soc Rev. 2010;39:455–63.
9. Li J-L, Liu X-Y. Architecture of supramolecular soft functional materials: from understanding to micro-/nanoscale engineering. Adv Funct Mater. 2010;20:3196–216.
10. John G, Shankar BV, Jadhav SR, Vemula PK. Biorefinery: a design tool for molecular gelators. Langmuir. 2010;26:17843–51.
11. Svobodová H, Noponen V, Kolehmainen E, Sievänen E. Recent advances in steroidal supramolecular gels. RSC Adv. 2012;2:4985–5007.
12. Babu SS, Prasanthkumar S, Ajayaghosh A. Self-assembled gelators for organic electronics. Angew Chem, Int Ed. 2012;51:1766–76.
13. Tam AY-Y, Yam VW-W. Recent advances in metallogels. Chem Soc Rev. 2013;42:1540–67.
14. Raeburn J, Cardoso AZ, Adams DJ. The importance of the self-assembly process to control mechanical properties of low molecular weight hydrogels. Chem Soc Rev. 2013;42:5143–56.
15. Yu G, Yan X, Han C, Huang F. Characterization of supramolecular gels. Chem Soc Rev. 2013;42:6697–722.
16. Segarra-Maset MD, Nebot VJ, Miravet JF, Escuder B. Control of molecular gelation by chemical stimuli. Chem Soc Rev. 2013;42:7086–98.
17. Babu SS, Praveen VK, Ajayaghosh A. Functional π-gelators and their applications. Chem Rev. 2014;114:1973–2129. (2014)
18. Kumar DK, Steed JW. Supramolecular gel phase crystallization: orthogonal self-assembly under non-equilibrium conditions. Chem Soc Rev. 2014;43:2080–8.
19. Praveen VK, Ranjith C, Armaroli N. White-light-emitting supramolecular gels. Angew Chem Int Ed. 2014;53:365–8.
20. Lan Y, Corradini MG, Weiss RG, Raghavanc SR, Rogers MA. To gel or not to gel: Correlating molecular gelation with solvent parameters. Chem Soc Rev. 2015;44:6035–58.
21. Li X, Li J, Gao Y, Kuang Y, Shi J, Xu B. Molecular nanofibers of olsalazine form supramolecular hydrogels for reductive release of an anti-inflammatory agent. J Am Chem Soc. 2010;132:17707–9.
22. Li J, Gao Y, Kuang Y, Shi J, Du X, Wang H, Yang Z, Xu B. Dephosphorylation of d-peptide derivatives to form biofunctional, supramolecular nanofibers/hydrogels and their potential applications for intracellular imaging and intratumoral chemotherapy. J Am Chem Soc. 2013;135:9907–14.
23. Silva GA, Czeisler C, Niece KL, Beniash E, Harrington DA, Kessler JA, Stupp SI. Selective differentiation of neural progenitor cells by high-epitope density nanofibers. Science. 2004;303:1352–5.
24. Matsumoto S, Yamaguchi S, Ueno S, Komatsu H, Ikeda M, Ishizuka K, Iko Y, Tabata KV, Aoki H, Ito S, Noji H, Hamachi I. Photo gel-sol/sol-gel transition and its patterning of a supramolecular hydrogel as stimuli-responsive biomaterials. Chem Eur J. 2008;14:3977–86.
25. Bekas DG, Tsirka K, Baltzis D, Paipetis AS. Self-healing materials: a review of advances in materials, evaluation, characterization and monitoring techniques. Compo Part B-Eng. 2016;87:92–119.

26. Klaewklod A, Tantishaiyakul V, Hirun N, Sangfai T, Li L. Characterization of supramolecular gels based on β-cyclodextrin and polyethyleneglycol and their potential use for topical drug delivery. Mater Sci Eng C. 2015;50:242–50.
27. Song Y, Gao J, Xu X, Zhao H, Xue R, Zhou J, Hong W, Qiu H. Fabrication of thermal sensitive folic acid based supramolecular hybrid gels for injectable drug release gels. Mater Sci Eng C. 2017;75:706–13.
28. Chronopoulou L, Togna AR, Guarguaglini G, Masci G, Giammarco F, Togna GI, Palocci C. Self-assembling peptide hydrogels promote microglial cells proliferation and NGF production. Soft Matter. 2012;8:5784–90.
29. Lin BF, Megley KA, Viswanathan N, Krogstad DV, Drews LB, Kade MJ, Qian Y, Tirrell MV. pH-responsive branched peptide amphiphile hydrogel designed for applications in regenerative medicine with potential as injectable tissue scaffolds. J Mater Chem. 2012;22:19447–54.
30. Murata K, Aoki M, Nishi T, Ikeda A, Shinkai S. New cholesterol-based gelators with light-and metal-responsive functions. Chem Commun. 1991;1991:1715–8.
31. de Jong JJD, Lucas LN, Kellogg RM, van Esch JH, Feringa BL. Reversible optical transcription of supramolecular chirality into molecular chirality. Science. 2004;304:278–81.
32. Chen J, Wu W, McNeil AJ. Detecting a peroxide-based explosive via molecular gelation. Chem Commun. 2012;48:7310–2.
33. Xue P, Xu Q, Gong P, Qian C, Ren A, Zhang Y, Lu R. Fibrous film of a two-component organogel as a sensor to detect and discriminate organic amines. Chem Commun. 2013;49:5838–40.
34. Tu T, Fang WW, Sun ZM. Visual-size molecular recognition based on gels. Adv Mater. 2013;25:5304–13.
35. Ono Y, Nakashima K, Sano M, Kanekiyo Y, Inoue K, Hojo J, Shinkai S. Organic gels are useful as a template for the preparation of hollow fiber silica. Chem Commun. 1998;1998:1477–8.
36. Basit H, Paul A, Sen S, Bhattacharya S. Two-component hydrogels comprising fatty acids and amines: Structure, properties, and application as a template for the synthesis of metal nanoparticles. Chem -Eur J. 2008;14:6534–45.
37. Kobayashi K, Hanabusa K, Hamasaki K, Kimura M, Shirai H, Shinkai S. Preparation of TiO2 hollow-fibers using supramolecular assemblies. Chem Mater. 2000;12:1523–5.
38. Kobayashi S, Hamasaki N, Suzuki M, Kimura M, Shirai H, Hanabusa K. Preparation of helical transition-metal oxide tubes using organogelators as structure-directing agents. J Am Chem Soc. 2002;124:6550–1.
39. Yang Y, Suzuki M, Fukui H, Shirai H, Hanabusa K. Preparation of helical mesoporous silica and hybrid silica nanofibers using hydrogelator. Chem Mater. 2006;18:1324–9.
40. Kubo W, Kambe S, Nakade S, Kitamura T, Hanabusa K, Wada Y, Yanagida S. Photocurrent-determining processes in quasi-solid-state dye-sensitized solar cells using ionic gel electrolytes. J Phys Chem B. 2003;107:4374–81.
41. Hanabusa K, Hiratsuka K, Kimura M, Shirai H. Easy preparation and useful character of organogel electrolytes based on low molecular weight gelator. Chem Mater. 1999;11:649–55.
42. Kartha KK, Babu SS, Srinivasan S, Ajayaghosh A. Attogram sensing of trinitrotoluene with a self-assembled molecular gelator. J Am Chem Soc. 2012;134:4834–41.
43. Dey N, Samanta SK, Bhattacharya S. Selective and efficient detection of nitro-aromatic explosives in multiple media including water, micelles, organogel, and solid support. ACS Appl Mater Interf. 2013;5:8394–400.
44. Hanabusa K, Takata S, Fujisaki M, Nomura Y, Suzuki M. Fluorescent gelators for detection of explosives. Bull Chem Soc Jpn. 2016;89:1391–401.
45. Cao X, Zhao N, Lv H, Ding Q, Gao A, Jing Q, Yi T. Strong blue emissive supramolecular self-assembly system based on naphthalimide derivatives and its ability of detection and removal of 2,4,6-trinitrophenol. Langmuir. 2017;33:7788–98.
46. Chen QJ, Fan FC, Long DH, Liu XJ, Liang XY, Qiao WM, Ling LC. Poly(ethyleneimine)-loaded silica monolith with a hierarchical pore structure for H2S adsorptive removal. Ind Eng Chem Res. 2010;49:11408–14.
47. Jing P, Fang XH, Yan JL, Guo J, Fang Y. Ultra-low density porous polystyrene monolith: Facile preparation and superior application. J Mater Chem A. 2013;1:10135–41.
48. Su F, Bray CL, Tan B, Cooper AI. Rapid and reversible hydrogen storage in clathrate hydrates using emulsion-templated polymers. Adv Mater. 2008;20:2663–6.
49. Furukawa H, Yaghi OM. Storage of hydrogen, methane, and carbon dioxide in highly porous covalent organic frameworks for clean energy applications. J Am Chem Soc. 2009;131:8875–83.
50. Furukawa H, Gandara F, Zhang YB, Jiang J, Queen WL, Hudson MR, Yaghi OM. Water adsorption in porous metal-organic frameworks and related materials. J Am Chem Soc. 2014;136:4369–81.
51. Gandara F, Furukawa H, Lee S, Yaghi OM. High methane storage capacity in aluminum metal-organic frameworks. J Am Chem Soc. 2014;136:5271–4.
52. Silverstein MS. PolyHIPEs: Recent advances in emulsion-templated porous polymers. Prog Polym Sci. 2014;39:199–234.
53. Huš S, Krajnc P. PolyHIPEs from methyl methacrylate: Hierarchically structured microcellular polymers with exceptional mechanical properties. Polym (Guildf). 2014;55:4420–4.
54. Wang B, Liang WX, Guo ZJ, Liu WM. Biomimetic super-lyophobic and super-lyophilic materials applied for oil/water separation: A new strategy beyond nature. Chem Soc Rev. 2015;44:336–61.
55. Binks BP. Macroporous silica from solid-stabilized emulsion templates. Adv Mater. 2002;14:1824–7.
56. Zhang YJ, Wang SP, Mohammad E, Motamedi M, Kotov NA. Inverted-colloidal-crystal hydrogel matrices as three-dimensional cell scaffolds. Adv Funct Mater. 2005;15:725–31.
57. Ma H, Hu J, Ma PX. Polymer scaffolds for small-diameter vascular tissue engineering. Adv Funct Mater. 2010;20:2833–41.
58. Hua Y, Chu YQ, Zhang SM, Zhu Y, Chen JD. Macroporous materials from water-in-oil high internal phase emulsion stabilized solely by water-dispersible copolymer particles. Polym. 2013;54:5852–7.
59. Hu Y, Gu XY, Yu Y, Jian H, Huang J, Hu M, Chen WK, Tong Z, Wang CY. Facile fabrication of poly(L-lactic acid)-grafted hydroxyapatite/poly(lactic-co-glycolic acid) scaffolds by pickering high internal phase emulsion templates. ACS Appl Mater Interfaces. 2014;6:17166–75.
60. Andersson J, Rosenholm J, Areva S, Lindén M. Influences of material characteristics on ibuprofen drug loading and release profiles from ordered micro- and mesoporous silica matrices. Chem Mater. 2004;16:4160–7.
61. Pierre SJ, Thies JC, Dureault A, Cameron NR, Hest JCM, Carette N, Michon T, Weberskirch R. Covalent enzyme immobilization onto photopolymerized highly porous monoliths. Adv Mater. 2006;18:1822–6.
62. Zhang YG, Zhao L, Patra PK, Ying JY. Synthesis and catalytic applications of mesoporous polymer colloids in olefin hydrosilylation. Adv. Synth Catal. 2010;350:662–6.
63. Chan-Thaw CE, Villa A, Katekomol P, Su D, Thomas A, Prati L. Covalent triazine framework as catalytic support for liquid phase reaction. Nano Lett. 2010;10:537–41.
64. Hayward AS, Eissa AM, Maltman DJ, Sano N, Przyborski SA, Cameron NR. Galactose-functionalized polyHIPE scaffolds for use in routine three dimensional culture of mammalian hepatocytes. Biomacromolecules. 2013;14:4271–7.

65. Kovacic S, Anzlovar A, Erjavec B, Kapun G, Matsko NB, Zigon M, Zagar E, Pintar A, Slugovc C. Macroporous ZnO foams by high internal phase emulsion technique: Synthesis and catalytic activity. ACS Appl Mater Interf. 2014;6:19075–81.
66. Tokuyama H, Sumida H, Kanehara A, Nii S. Effect of surfactants on the porous structure of poly(N-isopropylacrylamide) hydrogels prepared by an emulsion templating method. Colloid Polym Sci. 2009;287:115–21.
67. Tokuyama H, Kanehara A. Novel synthesis of macroporous poly (N-isopropylacrylamide) hydrogels using oil-in-water emulsions. Langmuir. 2007;23:11246–51.
68. Yu S, Tan H, Wang J, Liu X, Zhou K. High porosity super-macroporous polystyrene materials with excellent oil-water separation and gas permeability properties. ACS Appl Mater Interf. 2015;7:6745–53.
69. Zhang N, Jiang W, Wang T, Gu J, Zhong S, Zhou S, Xie T, Fu J. Facile preparation of magnetic poly(styrene-divinylbenzene) foam and its application as an oil absorbent. Ind Eng Chem Res. 2015;54:11033–9.
70. Miao Q, Chen X, Liu L, Peng J, Fang Y. Synergetic effect based gel-emulsions and their utilization for the template preparation of porous polymeric monoliths. Langmuir. 2014;30:13680–8.
71. Hanabusa K, Ueda T, Takata S, Suzuki M. Synthesis of fluorescent gelators and direct observation of gelation with a fluorescence microscope. Chem Eur J. 2016;22:16939–49.